



同濟大學  
TONGJI UNIVERSITY

博士学位论文

新型纳米结构材料的设计合成  
及其电容性能研究

姓 名：王欢文

学 号：1110507

所在院系：理学部化学系

学科门类：化学

学科专业：物理化学

指导教师：王雪峰 教授

二〇一四年五月



同濟大學  
TONGJI UNIVERSITY

A dissertation submitted to  
Tongji University in conformity with the requirements for  
the degree of Doctor of Philosophy

**Design and synthesis of novel  
nanostructured materials for supercapacitors**

Candidate: Huanwen Wang

Student Number: 1110507

School/Department: Chemistry Department

Discipline: Chemistry

Major: Physical Chemistry

Supervisor: Prof Xuefeng Wang

May, 2014

## 学位论文版权使用授权书

本人完全了解同济大学关于收集、保存、使用学位论文的规定，同意如下各项内容：按照学校要求提交学位论文的印刷本和电子版；学校有权保留学位论文的印刷本和电子版，并采用影印、缩印、扫描、数字化或其它手段保存论文；学校有权提供目录检索以及提供本学位论文全文或者部分的阅览服务；学校有权按有关规定向国家有关部门或者机构送交论文的复印件和电子版；在不以赢利为目的的前提下，学校可以适当复制论文的部分或全部内容用于学术活动。

学位论文作者签名：

年 月 日

# 同济大学学位论文原创性声明

本人郑重声明：所提交的学位论文，是本人在导师指导下，进行研究工作所取得的成果。除文中已经注明引用的内容外，本学位论文的研究成果不包含任何他人创作的、已公开发表或者没有公开发表的作品的内容。对本论文所涉及的研究工作做出贡献的其他个人和集体，均已在文中以明确方式标明。本学位论文原创性声明的法律责任由本人承担。

学位论文作者签名：

年 月 日

## 摘要

当今世界对化石燃料的过度依赖不但使这一有限资源即将枯竭,而且也给地球环境带来巨大危害。于是,科学工作者对各种清洁或绿色能源技术寄予了前所未有的厚望。超级电容器,是近年来出现的一种新型储能器件,以其超高比功率和良好循环寿命而著称,但较低的能量密度一直是制约其应用的瓶颈。到目前为止,该问题的解决途径主要包括:(1)构建特定取向的纳米结构,具有比本体材料更优异的储能性质,例如一维(纳米线,纳米管,纳米带,纳米纤维等)、二维(纳米片,纳米壁等)、三维多层次孔状结构;(2)设计复合材料,体现各种组分的协同性能,例如碳/金属氧化物、碳/导电聚合物、碳/氧化物/聚合物。本论文在广泛文献调研的基础上,利用脉冲激光沉积等方法设计和合成了一系列新型纳米结构电极材料,并研究了其电容性能,主要内容概括如下:

(1)在氧气气氛下,脉冲激光溅射镍金属靶,产生的等离子体羽流与氧分子反应生成氧化镍,直接沉积在导电基底上。通过采用X射线衍射(XRD)、拉曼光谱(Raman spectra)、场发射扫描电镜(FESEM)对复合物进行物理表征,所形成的氧化镍薄膜呈现多孔结构,有利于电解质离子传输。电化学测试表明,该氧化镍薄膜电极具有较好的电容特性,在 $1\text{ A g}^{-1}$ 时,比电容达 $835\text{ F g}^{-1}$ 。在电流密度高达 $40\text{ A g}^{-1}$ 时,电容保持率为59%(相对于 $1\text{ A g}^{-1}$ )。此外,该氧化镍薄膜电极具有良好的循环寿命,在1000次充放电循环后,电容仅衰减了6%。

(2)在臭氧气氛下,脉冲激光溅射锰金属靶,产生的等离子体羽流与臭氧分子反应生成二氧化锰,直接沉积在导电基底上。材料表征结果显示,二氧化锰薄膜以超薄(10 nm)纳米片阵列形式垂直于基底。该二氧化锰纳米片阵列可以直接作为超级电容器电极,电化学测试表明,该阵列电极具有优异的倍率性能(在 $100\text{ A g}^{-1}$ 时,电容保持率为52%);较高的比电容(在 $1\text{ A g}^{-1}$ 时,比电容为 $337\text{ F g}^{-1}$ );良好的循环寿命(在6000次循环后电容没有衰减)。

(3)利用脉冲激光沉积技术,将氧化镍薄膜直接沉积在三维高导电性的石墨烯泡沫上,由于石墨烯的高导电性和泡沫的多孔性非常有利于快速的电子传导和离子传输,该氧化镍/石墨烯泡沫电极在三电极体系中具有很高的电容值( $2\text{ A g}^{-1}$ 时为 $1225\text{ F g}^{-1}$ )和出色的倍率性能(在 $100\text{ A g}^{-1}$ 时,电容保持率为68%)。在KOH水溶液中,以氧化镍/石墨烯泡沫作为正极,多孔氮掺杂的碳纳米管为负极,构建了一种新型的不对称超级电容器。在0.0~1.4 V的电位窗口下,当功率密度为 $700\text{ W kg}^{-1}$ 时,能量密度高达 $32\text{ W h kg}^{-1}$ 。特别是在2.8 s充放电倍率( $42\text{ kW kg}^{-1}$ )下,能量密度仍保持有 $17\text{ W h kg}^{-1}$ 。同时,该不对称电容器具有优秀的循

环稳定性（2000 次循环后，电容保持率达 94%）。

（4）利用水热法在柔性的碳布基底上控制合成了钴酸镍纳米线和纳米片。在相同负载量的情况下，纳米线和纳米片呈现出了截然不同的电容性能。测试结果表明，相比于纳米片形貌，纳米线形貌具有更高的比电容值和循环性能。这种不同形貌之间的对比揭示了电化学能量储存中的“过程-结构-性质”的关系。

（5）利用 Hummers 法将多壁碳纳米管同时沿着横向和纵向剪切为卷曲的石墨烯纳米片。这种卷曲的石墨烯片具有一维纳米管和二维石墨烯的杂化结构。电化学测试表明，相比于原始的多壁碳纳米管，卷曲的石墨烯片在酸性、碱性和中性电解质中均表现出更高的电容性能。例如，在  $0.3 \text{ A g}^{-1}$  时，比电容在碱性电解质中达到  $256 \text{ F g}^{-1}$ 。剪切后电容的增加，主要归因于较高的电解质润湿性、缺陷密度和比表面积。同时，本章也提供了一种大规模合成石墨烯的途径。这种卷曲的石墨烯片有望应用于其他领域，例如传感器，电池材料和气体储存等。

（6）以五氧化二钒和氧化石墨为原料，通过一步法合成了三维石墨烯/二氧化钒纳米带复合物凝胶。在凝胶形成过程中，一维二氧化钒纳米带和二维石墨烯片通过氢键自组装成交联多孔的微结构。由于这种多孔凝胶结构和纳米带赝电容贡献，石墨烯/二氧化钒纳米带复合物凝胶在  $-0.6 \sim 0.6 \text{ V}$  电位窗口下，比电容在  $1 \text{ A g}^{-1}$  时达到  $426 \text{ F g}^{-1}$ ，远大于相同测试条件下的单组分的电容值（ $191 \text{ F g}^{-1}$  和  $243 \text{ F g}^{-1}$ ）。此外，由于组分间的正协同效应，复合物凝胶电极表现出更高的倍率性能和循环稳定性。

（7）为了增加超级电容器的能量密度，现有的研究主要集中于正极材料，而负极材料很少有人研究。在本章，单晶的三氧化二铁纳米粒子直接生长在石墨烯凝胶上，作为高性能的超级电容器负极材料。在三氧化二铁/石墨烯复合物凝胶形成过程中，三氧化二铁纳米粒子与石墨烯片通过氢键作用自组装形成高表面积多孔结构。在  $-1.05 \sim -0.3 \text{ V}$  电位窗口下，复合物凝胶具有高比电容（在  $2 \text{ A g}^{-1}$  时为  $908 \text{ F g}^{-1}$ ）和优异的倍率性能（在  $100 \text{ A g}^{-1}$  时，电容保持率为 68%）。另外，相比于单纯的三氧化二铁，复合物凝胶的稳定性也有明显的提高。

（8）为了进一步提高超级电容器能量密度，本章以石墨烯凝胶为正极、二氧化钛纳米带为负极、 $\text{LiPF}_6/\text{EC-DMC}$  为有机电解质构建了一种新型的杂化电容器。由于石墨烯凝胶的多孔性、高导电性和二氧化钛独特的纳米带阵列结构，杂化电容器有利于快速的离子和电子的传输。在  $0.0 \sim 3.8 \text{ V}$  电位窗口下，能量密度高达  $82 \text{ Wh kg}^{-1}$ 。甚至在  $8.4 \text{ s}$  充放电倍率下，能量密度仍保持有  $21 \text{ Wh kg}^{-1}$ 。这些测试结果表明，该杂化电容器具有比超级电容器更高的能量密度和比锂离子电池更高的功率密度。

**关键词：**超级电容器，脉冲激光沉积，电极材料，能量，功率，电容，稳定性

## ABSTRACT

The ever worsening energy depletion and global warming issues call for not only urgent development of clean alternative energies and emission control of global warming gases, but also more advanced energy storage and management devices. Supercapacitor, as a new type of energy storage devices, has triggered intense research due to its ultrahigh power density and long cycle life, but its lower energy density in comparasion with secondary batteries is a bottleneck in pratical application. So far, many efforts have been made to improve the energy density by creating nanostructures, such as 1D (nanowires, nanotubes, nanobelts, nanofibres), 2D (nanosheets, nanowalls), and 3D hierarchical porous structures, which display higher specific capacitances than their bulk counterparts, or composites between different kinds of nanomaterials, such as carbon/metal oxide, carbon/conducting polymers, and carbon/metal oxide/conducting polymers, which can indicate synergistic effects. In the present work, we design and synthesize a series of novel nanostructured materials for supercapacitors on the basis of previous references. The main is as follows:

(1) This work reports the pulsed laser reactive deposition of the NiO thin film by ablating nickel targets in lowpressure O<sub>2</sub> atmosphere at room temperature. The electrode exhibits a porous structure, which facilitates ion transport in the electrode/electrolyte. When applied as an electrode, the porous NiO film exhibits the high specific capacitance (835 F g<sup>-1</sup> at 1 A g<sup>-1</sup>). Meanwhile, the film exhibits a superb rate capability. At a very high current density of 40 A g<sup>-1</sup> there is more than 59% retention in the capacitance relative to 1 A g<sup>-1</sup>. Furthermore, the excellent cycling performance (94% capacitance retention after 1000 cycles) is achieved for the film electrode. These results demonstrate that pulsed laser deposition (PLD) is a very promising technique for making the film electrodes for applications in electrochemical energy storage.

(2) A pulsed laser deposition process using ozone as an oxidant is developed to synthesize manganese oxide nanosheet arrays, which display excellent rate capability (52% capacity retention at 100 A g<sup>-1</sup>), comparable capacitance (337 F g<sup>-1</sup> at 1 A g<sup>-1</sup>) and long cycle life (without degradation after 6000 cycles).

(3) A pulsed laser deposition process using ozone as an oxidant is developed to grow NiO nanoparticles on highly conductive three-dimensional (3D) graphene foam

(GF). The excellent electrical conductivity and interconnected pore structure of the hybrid NiO/GF electrode facilitate fast electron and ion transportation. The NiO/GF electrode displays a high specific capacitance ( $1225 \text{ F g}^{-1}$  at  $2 \text{ A g}^{-1}$ ) and a superb rate capability (68% capacity retention at  $100 \text{ A g}^{-1}$ ). A novel asymmetric supercapacitor with high power and energy densities is successfully fabricated using NiO/GF as the positive electrode and hierarchical porous nitrogen-doped carbon nanotubes (HPNCNTs) as the negative electrode in aqueous KOH solution. Because of the high individual capacitive performance of NiO/GF and HPNCNTs, as well as the synergistic effect between the two electrodes, the asymmetric capacitor exhibits an excellent energy storage performance. At a voltage range from 0.0 to 1.4 V, an energy density of  $32 \text{ W h kg}^{-1}$  is achieved at a power density of  $700 \text{ W kg}^{-1}$ . Even at a 2.8 s charge–discharge rate ( $42 \text{ kW kg}^{-1}$ ), an energy density as high as  $17 \text{ W h kg}^{-1}$  is retained. Additionally, the NiO/GF//HPNCNT asymmetric supercapacitor exhibits excellent cycling durability, with 94% specific capacitance retained after 2000 cycles.

(4) Controllable synthesis and high yield of functional nanomaterials on conductive substrates are highly desirable for energy conversion and storage applications. In this work, two different porous  $\text{NiCo}_2\text{O}_4$  nanoarchitectures (including nanowires and nanosheets) are directly grown on carbon cloth collectors, which display a structure-dependence in their capacitive behaviors. Our results show that the nanowire morphology exhibits higher specific capacitance and better cycling performance in the three-electrode configuration. The pseudocapacitive difference is related to the surface area and pore structure of  $\text{NiCo}_2\text{O}_4$  nanocrystals. This comparison among different morphologies reveals a process–structure–property relationship in electrochemical energy storage.

(5) We report a remarkable transformation of multiwalled carbon nanotubes (MWCNTs) to curved graphene nanosheets (CGN) by the Hummers method. Through this simple process, MWCNTs can be cut and unzipped in the transverse and longitudinal directions, respectively. The as-obtained CGN possess the unique hybrid structure of 1D nanotube and 2D graphene. Such a particular structure together with the improved effective surface area affords high specific capacitance and good cycling stability during the charge–discharge process when used as supercapacitor electrodes. The electrochemical measurements show that CGN exhibit higher capacitive properties than pristine MWCNTs in three different types of aqueous electrolytes, 1 M KOH, 1 M  $\text{H}_2\text{SO}_4$ , and 1 M  $\text{Na}_2\text{SO}_4$ . A specific capacitance of as high as  $256 \text{ F g}^{-1}$  at

a current density of  $0.3 \text{ A g}^{-1}$  is achieved over the CGN material. The improved capacitance may be attributed to high accessibility to electrolyte ions, extended defect density, and increased effective surface area. Meanwhile, this high-yield production of graphene from low cost MWCNTs is important for the scalable synthesis and industrial application of graphene. Furthermore, this novel CGN nanostructure could also be promisingly applied in many fields such as nanoelectronics, sensors, nanocomposites, batteries, and gas storage.

(6) A facile one-step strategy has been developed to prepare 3D graphene/ $\text{VO}_2$  nanobelt composite hydrogels, which can be readily scaled-up for mass production by using commercial  $\text{V}_2\text{O}_5$  and graphene oxide as precursors. During the formation of the graphene/ $\text{VO}_2$  architecture, 1D  $\text{VO}_2$  nanobelts and 2D flexible graphene sheets are self-assembled to form interconnected porous microstructures through hydrogen bonding, which facilitates charge and ion transport in the electrode. Due to the hierarchical network framework and the pseudocapacitance contribution from  $\text{VO}_2$  nanobelts, the hybrid electrode demonstrates excellent capacitive performances. In the two-electrode configuration, the graphene/ $\text{VO}_2$  nanobelt composite hydrogel exhibits a specific capacitance of  $426 \text{ F g}^{-1}$  at  $1 \text{ A g}^{-1}$  in the potential range of  $-0.6$  to  $0.6 \text{ V}$ , which greatly surpasses that of each individual counterpart ( $191 \text{ F g}^{-1}$  and  $243 \text{ F g}^{-1}$  at  $1 \text{ A g}^{-1}$  for  $\text{VO}_2$  nanobelt and graphene hydrogel, respectively). The hybrid electrode also shows an improved rate capability and cycling stability, which is indicative of a positive synergistic effect of  $\text{VO}_2$  and graphene on the improvement of electrochemical performance. These findings reveal the importance and great potential of graphene composite hydrogels in the development of energy storage devices with high power and energy densities.

(7) To increase the energy density of supercapacitors to approach that of batteries, the current research is always directed towards the cathode materials, whereas the anode materials are rarely studied. In the present work, single-crystalline  $\text{Fe}_2\text{O}_3$  nanoparticles directly grown on graphene hydrogels are investigated as high performance anode materials for supercapacitors. During the formation of the graphene/ $\text{Fe}_2\text{O}_3$  composite hydrogels, flexible graphene sheets decorated with  $\text{Fe}_2\text{O}_3$  particles are self-assembled to form interconnected porous microstructures with high specific surface area, which strongly facilitate charge and ion transport in the full electrode. Infrared spectra show that hydrogen bond is formed between C-OH on graphene hydrogels and  $\text{Fe}_2\text{O}_3$ . Benefits from the combined graphene hydrogels and

Fe<sub>2</sub>O<sub>3</sub> particles in such a unique structure are that the graphene/Fe<sub>2</sub>O<sub>3</sub> composite electrode exhibits an ultrahigh specific capacitance of 908 F g<sup>-1</sup> at 2 A g<sup>-1</sup> within the potential range from -1.05 to -0.3 V, and an outstanding rate capability (69% capacity retention at 50 A g<sup>-1</sup>). Furthermore, the cycling performance is clearly much better for the graphene/Fe<sub>2</sub>O<sub>3</sub> composite hydrogels than that for pure Fe<sub>2</sub>O<sub>3</sub> sample. These findings open a new pathway to the design and fabrication of three-dimensional graphene hydrogel composites as anode materials in the development of high-performance energy-storage systems.

(8) A novel hybrid Li-ion capacitor with high energy and power densities—combining an electrochemical double layer capacitor (EDLC) type cathode (graphene hydrogels) with a Li-ion battery type anode (TiO<sub>2</sub> nanobelt arrays)—has been constructed in a non-aqueous electrolyte. Benefiting from three dimensional (3D) porous network and high electrical conductivity of graphene hydrogel cathode (power source), free-standing TiO<sub>2</sub> nanobelt arrays growing directly on Ti foil as anodes without any ancillary materials (energy source), as well as the synergistic effect between the two electrodes, the hybrid Li-ion capacitor enables rapid electron and ion transport in electrochemical energy storage. Within a voltage range from 0.0 to 3.8 V, 82 Wh kg<sup>-1</sup> of energy is achieved at a power density of 570 W kg<sup>-1</sup>. Even at an 8.4-s charge/discharge rate, an energy density as high as 21 Wh kg<sup>-1</sup> can be retained. These results suggest that the TiO<sub>2</sub> nanobelt arrays//graphene hydrogels Li-ion capacitor exhibits higher energy density than supercapacitors and better power density than Li-ion batteries, which makes it attractive electrochemical power sources.

**Key words:** supercapacitor, pulsed laser deposition, electrode materials, energy, power, capacitance, stability

## 目录

摘要.....	I
ABSTRACT.....	III
目录.....	VII
第 1 章 绪论.....	1
1.1 超级电容器的组成和结构.....	1
1.2 超级电容器的基本原理和分类.....	2
1.3 超级电容器电极材料的研究进展.....	3
1.3.1 碳基材料.....	4
1.3.2 金属氧化物材料.....	8
1.3.3 导电聚合物材料.....	9
1.4 脉冲激光沉积技术在超级电容器中的应用.....	10
1.4.1 脉冲激光沉积基本原理.....	11
1.4.2 脉冲激光沉积实验装置.....	12
1.4.3 脉冲激光沉积技术特点.....	13
1.5 超级电容器性能的测试方法.....	13
1.5.1 循环伏安法.....	13
1.5.2 恒电流充放电测试.....	17
1.5.3 电化学交流阻抗测试.....	18
1.5.4 其他测试方法.....	19
1.6 纳米尺度下的超级电容器与二次电池的异同点.....	19
1.7 论文选题依据.....	21
1.8 论文主要内容.....	21
第 2 章 室温下脉冲激光沉积多孔氧化镍薄膜及其高倍率赝电容性质的研究.....	23
2.1 引言.....	23
2.2 实验部分.....	23
2.2.1 实验原料与仪器.....	23
2.2.2 材料制备.....	24
2.2.3 材料表征.....	25
2.2.3.1 物理表征.....	25
2.2.3.2 电化学表征.....	25
2.3 结果与讨论.....	25
2.4 本章小结.....	28
第 3 章 脉冲激光沉积大面积二氧化锰纳米片阵列及其在超级电容器中的应用.....	29
3.1 引言.....	29

3.2 实验部分.....	29
3.2.1 实验原料与仪器.....	29
3.2.2 材料制备.....	30
3.2.3 材料表征.....	30
3.2.3.1 物理表征.....	30
3.2.3.2 电化学表征.....	30
3.3 结果与讨论.....	30
3.4 本章小结.....	35
第4章 构建基于氧化镍/石墨烯泡沫和多孔氮掺杂碳纳米管的不对称超级电容器及其超高的倍率性能.....	37
4.1 引言.....	37
4.2 实验部分.....	38
4.2.1 实验原料与仪器.....	38
4.2.2 材料的制备.....	38
4.2.2.1 氧化镍/石墨烯泡沫的合成.....	38
4.2.2.2 多孔氮掺杂碳纳米管的合成.....	39
4.2.3 材料表征.....	39
4.2.3.1 物理表征.....	39
4.2.3.2 电化学表征.....	39
4.3 结果与讨论.....	40
4.3.1 正极材料.....	40
4.3.2 负极材料.....	44
4.3.3 不对称超级电容器.....	48
4.4 本章小结.....	49
第5章 控制生长钴酸镍纳米线和纳米片在碳布上及其不同的赝电容行为.....	51
5.1 引言.....	51
5.2 实验部分.....	51
5.2.1 实验原料与仪器.....	52
5.2.2 材料的制备.....	52
5.2.3 材料表征.....	52
5.2.3.1 物理表征.....	52
5.2.3.2 电化学表征.....	52
5.3 结果与讨论.....	53
5.3.1 NiCo <sub>2</sub> O <sub>4</sub> 纳米线和纳米片的合成过程.....	53
5.3.2 材料表征.....	54
5.3.3 电化学表征.....	56
5.4 本章小结.....	58
第6章 剪切多壁碳纳米管为弯曲石墨烯纳米片及其增强的电容性能.....	60

6.1 引言.....	60
6.2 实验部分.....	60
6.2.1 实验原料与仪器.....	60
6.2.2 材料的制备.....	61
6.2.3 材料表征.....	61
6.2.3.1 物理表征.....	61
6.2.3.2 电化学表征.....	61
6.3 结果与讨论.....	61
6.4 本章小结.....	67
第 7 章 三维的石墨烯/二氧化钒纳米带复合物凝胶的制备与电化学表征 .....	69
7.1 引言.....	69
7.2 实验部分.....	70
7.2.1 实验原料与仪器.....	70
7.2.2 材料的制备.....	70
7.2.3 材料表征.....	70
7.2.3.1 物理表征.....	71
7.2.3.2 电化学表征.....	71
7.3 结果与讨论.....	71
7.4 本章小结.....	82
第 8 章 单晶的三氧化二铁纳米粒子生长在石墨烯凝胶作为超级电容器负极材料 .....	84
8.1 引言.....	84
8.2 实验部分.....	85
8.2.1 实验原料与仪器.....	85
8.2.2 材料的制备.....	85
8.2.3 材料表征.....	85
8.2.3.1 物理表征.....	85
8.2.3.2 电化学表征.....	86
8.3 结果与讨论.....	86
8.4 本章小结.....	94
第 9 章 基于石墨烯凝胶正极和二氧化钛纳米带阵列负极的杂化超级电容器的构建及其超高的能量密度.....	95
9.1 引言.....	95
9.2 实验部分.....	95
9.2.1 实验原料与仪器.....	95
9.2.2 材料的制备.....	96
9.2.3 材料表征.....	96
9.2.3.1 物理表征.....	96

9.2.3.2 电化学表征.....	96
9.3 结果与讨论.....	97
9.4 本章小结.....	103
第 10 章 结论与展望.....	104
10.1 结论.....	104
10.2 展望.....	104
致谢.....	105
参考文献.....	106
个人简历、在读期间发表的学术论文与研究成果.....	128

## 第1章 绪论

目前,世界各国都已投入极大财力、物力和人力发展新型电化学能量转换及贮存技术,并研制出许多高性能的化学电源。其中,超级电容器(Supercapacitors) [1, 2],是近年来出现的一种新型储能器件,也是绿色能源技术的重要组成部分。它与目前广泛使用的各种储能器件相比,其电荷存储能力远高于物理电容器,充放电速度和效率又优于一次或二次电池(图 1.1)。此外,超级电容器还具有对环境无污染、循环寿命长、使用温度范围宽、安全性能高等特点 [3]。它与氢动力汽车、混合动力汽车和电动汽车的发展密切相关。采用超级电容器和电池组合的方法,构成混合电源系统作为电动汽车的动力电源可以满足各种技术要求,启动加速时,主要是电容器放电;减速刹车时,可以由制动的充电系统给电容器充电,回收能量。这样可以降低电池的负荷峰值,延长电池寿命,提高能量的利用效率,因此,采用超大容量电容器/电池混合驱动系统被认为是解决电动汽车驱动的最佳方案之一。实际上,超级电容器的用途不仅限于此,它在通信、无线电电子技术、计算机电源、军事、航天领域以及人体医学等方面也有用武之地。

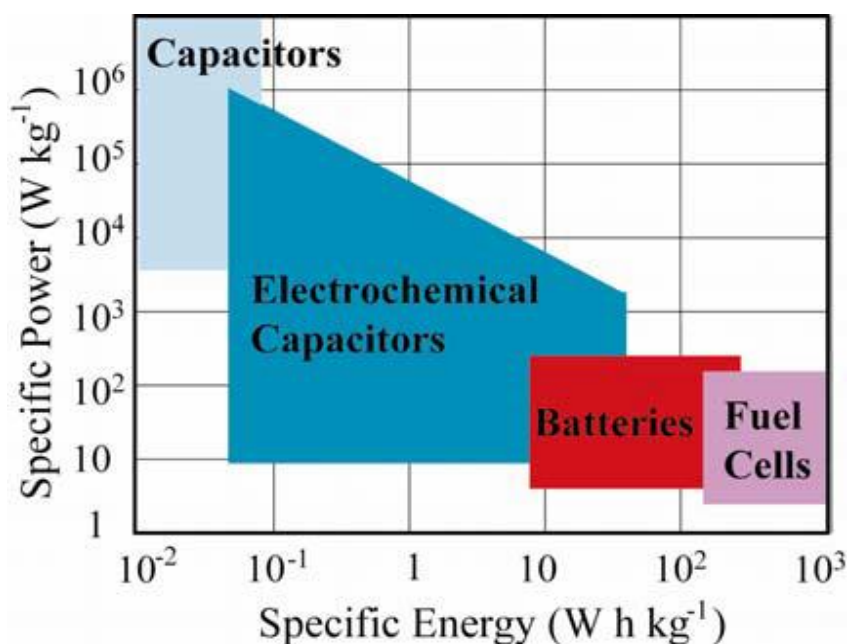


图 1.1 各种电化学能量储存装置的能量-功率图 [4]。

### 1.1 超级电容器的组成和结构

超级电容器和其他电化学储能设备在配置方面存在许多相同之处。通常，

超级电容器系统包含四个部分（图 1.2）：（a）正极，（b）负极，（c）电解液，（d）隔膜。在充电过程中，电解液中的阳离子（例如  $\text{Li}^+$ ， $\text{K}^+$ ， $\text{H}^+$ 等）或阴离子（例如  $\text{OH}^-$ 等）以扩散、迁移、吸/脱附等方式从一个电极运动至其对电极。同时，电子将沿着外电路从阴极流向阳极。在放电过程中，阴/阳离子从对电极脱出或解吸附，然后通过电解液回到原电极处；电子则从阳极流回阴极，通过外电路并对外做功。工作电极的制造技术、电解质的组成和隔离膜质量对超级电容器的性能有决定性的影响，电解质的分解电压决定超级电容器的工作电压。水溶液电解液电容器的工作电压在 1 V 左右，而有机电解液电容器的工作电压在 3 V 左右 [5]。

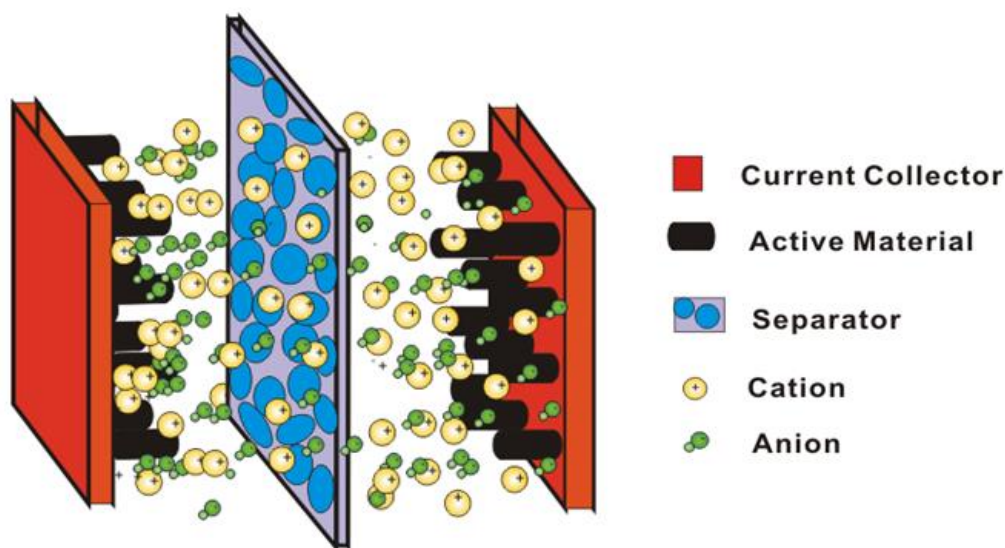


图 1.2 超级电容器示意图。

## 1.2 超级电容器的基本原理和分类

基于电荷存储机理（图1.3），超级电容器可以分为两类 [6, 7]：即双电层电容器（Electric double-layer capacitor）和氧化还原电容器（Redox capacitor）、也称赝（或准）电容器（Pseudocapacitor）。对于前者而言，能量的存储主要来源于高表面电极材料和电解质溶液接触界面处电荷（电子电荷或离子电荷）的有序分离；对于后者，在电极表面或体相中的电活性物质进行欠电位沉积，发生高度可逆的化学吸脱附或氧化还原反应（Faradaic reactions），产生与电极充电电位有关的赝（或准）电容，其储存电荷的过程不仅包括电极活性物质由于氧化还原反应而将电荷储存于电极中，而且包括电极材料表面与电解质之间的双电层电荷的储存。这种电极系统的电压随电荷转移的量呈线性变化，表现出电容的特征，故称为“准电容”。充电时，电解液中的离子（一般为  $\text{H}^+$  或  $\text{OH}^-$ ）在外加电场的作用

下由溶液中扩散到电极/溶液界面，而后通过界面的电化学反应而进入到电极表面活性氧化物的体相中；若电极材料是具有较大比表面积的氧化物，这样就会有相当多的电化学反应发生，大量的电荷就被存储在电极中。放电时这些进入氧化物中的离子又会重新返回到电解液中，同时所存储的电荷通过外电路而释放出来 [8, 9]。

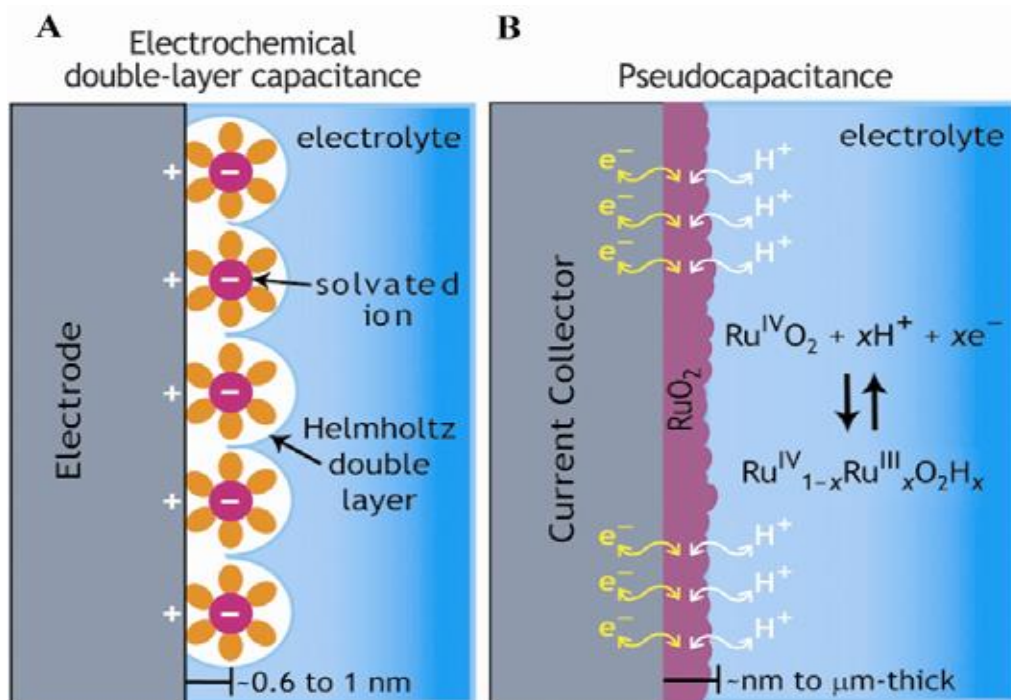


图 1.3 超级电容器电荷存储机理“示意图”：(A) 双电层电容 (B) 准电容 [4]。

### 1.3 超级电容器电极材料的研究进展

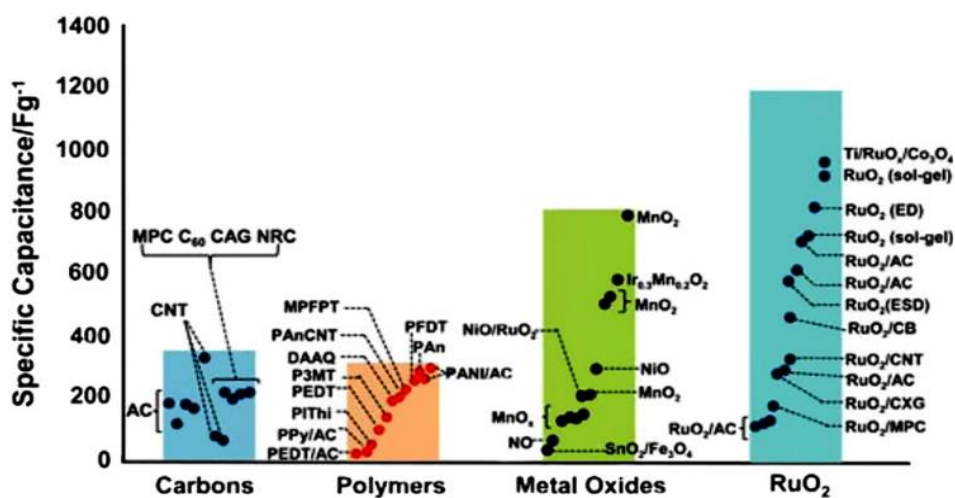


图 1.4 各种超级电容器电极材料的电容值 [4]。